# Cortical capacity constraints for visual working memory: dissociation of fMRI load effects in a fronto-parietal network

David E.J. Linden,[a,b,]* Robert A. Bittner,[b] Lars Muckli,[a] James A. Waltz,[a]
Nikolaus Kriegeskorte,[c] Rainer Goebel,[c] Wolf Singer,[a] and Matthias H.J. Munk[a]

[a] *Max–Planck–Institut für Himforschung, Deutschordenstrasse 46, D-60528 Frankfurt, Germany*
[b] *Laboratory for Neurophysiology and Neuroimaging, Department of Psychiatry, Johann Wolfgang Goethe-Universität,
Theodor-Stem-Kai 7, D-60590 Frankfurt, Germany*
[c] *Department of Cognitive Neuroscience, Faculty of Psychology, Maastricht University, Postbus 616, 6200MD Maastricht, The Netherlands*

## Abstract

Working memory (WM) capacity limitations and their neurophysiological correlates are of special relevance for the understanding of higher cognitive functions. Evidence from behavioral studies suggests that restricted attentional resources contribute to these capacity limitations. In an event-related functional magnetic resonance imaging (fMRI) study, we probed the capacity of the human visual WM system for up to four complex nonnatural objects using a delayed discrimination task. A number of prefrontal and parietal areas bilaterally showed increased blood oxygen level-dependent activity, relative to baseline, throughout the task when more than one object had to be held in memory. Monotonic increases in response to memory load were observed bilaterally in the dorsolateral prefrontal cortex (DLPFC) and the presupplementary motor area (pre-SMA). Conversely, activity in the frontal eye fields (FEFs) and in areas along the intraparietal sulcus (IPS) peaked when subjects had to maintain only two or three objects and decreased in the highest load condition. This dissociation of memory load effects on cortical activity suggests that the cognitive operations subserved by the IPS and FEF, which are most likely related to attention, fail to support visual WM when the capacity limit is approached. The correlation of brain activity with performance implies that only the operations performed by the DLPFC and pre-SMA, which support an integrated representation of visual information, helped subjects to maintain a reasonable level of performance in the highest load condition. These results indicate that at least two distinct cortical subsystems are recruited for visual WM, and that their interplay changes when the capacity limit is reached.
© 2003 Elsevier Inc. All rights reserved.

Working memory (WM) is thought to be an essential cognitive ability that allows the encoding and storing of information for short periods of time, thus making it available for manipulation and for the active guidance of behavior (Baddeley, 1992). Electrophysiological studies in monkeys (Fuster and Alexander, 1971; Funahashi et al., 1989; Miller et al., 1996; Pesaran et al., 2002) along with functional neuroimaging studies in humans (Cohen et al., 1997; Courtney et al., 1997; Smith and Jonides, 1999) have identified a distributed network of cortical areas engaged during

working memory tasks including areas in the dorsolateral and ventrolateral prefrontal cortex (DLPFC, VLPFC) and the superior and inferior parietal lobule (SPL, IPL). Whether these areas display a functional segregation according to the type of information to be stored remains controversial.

While some studies have found differences in the recruitment of dorsal and ventral lateral prefrontal areas for the storage of visuospatial and object features, respectively (for review, see Haxby et al., 2000; Levy and Goldman-Rakic, 2000), others have found such a segregation for the type of processing required (e.g., manipulation versus maintenance), rather than the memoranda (for review see Owen, 2000; D'Esposito et al., 2000). For the posterior cortex, a dissociation of visual stimulus processing into a dorsal (oc-

* Corresponding author. Max Planck Institute for Brain Research, Deutschordenstrasse 46, D-60528 Frankfurt, Germany. Fax: +49-69-96769-327.

*E-mail address:* linden@mpih-frankfurt.mpg.de (D.E.J. Linden).

cipitoparietal) stream for spatial and motion information and a ventral (occipitotemporal) stream for object characteristics has been confirmed in numerous studies on humans and nonhuman primates (for review see Ungerleider and Haxby, 1994). This dissociation has also been found in the encoding phase of human working memory studies (Munk et al., 2002), with inferior temporal areas more responsive to object features and parietal areas more responsive to locations. Regarding the delay phase of working memory tasks, sustained parietal activation was found when the spatial layout of a stimulus display had to be remembered (Munk et al., 2002), while sustained medial temporal activation was observed in a face memory task (Ranganath and D'Esposito, 2001). For other classes of visual objects, evidence for sustained temporal activation, as could be expected on the basis of monkey electrophysiology (Miller et al., 1993), is still lacking.

One central characteristic of working memory is its limited capacity. While Miller originally proposed that this capacity is seven plus or minus two chunks (Miller, 1994), a large body of evidence indicates that the actual storage size in humans is restricted to about four items (Luck and Vogel, 1997; Cowan, 2001; Wheeler and Treisman, 2002). Whereas functional imaging has contributed greatly to the question of where in the brain different classes and features of visual objects are stored and manipulated, the neurophysiological basis of working memory capacity limitations is still poorly understood. Functional imaging studies that used a parametric variation of memory load in n-back tasks (Braver et al., 1997; Cohen et al., 1997) have found corresponding increases in prefrontal activation. However, in order to distinguish the brain activation patterns related to encoding and retention with functional magnetic resonance imaging (fMRI), delayed discrimination tasks (DDTs) are often used in a trial-based design (Zarahn et al., 1997). A number of fMRI studies that varied the memory load of a DDT have also found increases of activity mainly in prefrontal areas (Rypma and D'Esposito, 1999; Rypma et al., 2002). Yet, it has been suggested that blood oxygen level-dependent (BOLD) activity might decline again under conditions of high WM demand (Callicott et al., 1999). Such an "inverted U-shape" response has also been implicated in the limitation of the capacity to shift visual attention (Beauchamp et al., 2001). A global decrease in activation in conditions of high memory or attentional demand is difficult to interpret because it might merely indicate that the subjects were not equally engaged by the task, perhaps due to frustration with their declining performance. Local decreases, however, especially when accompanied by continuous increases in other areas, could inform us about the localization of capacity constraints and potential compensatory strategy shifts.

A number of previous behavioral and neuroimaging studies provide indications of where in the WM network such decreases might be observed when the memory capacity limit is approached. Several models implicate restricted attentional resources as a cause for working memory capacity constraints (Cowan, 2001; Kane et al., 2001; Wheeler and Treisman, 2002). It has also been shown that visual attention is particularly sensitive to interference from working memory requirements in conditions of high memory load (de Fockert et al., 2001). One way to overcome limits in the sequential attentional scanning of visual objects would be to form symbolic representations of the visual material especially in the high memory load conditions. This would lead to increased prefrontal activation, which has also been reported for supracapacity verbal memory conditions (Rypma and Gabrieli, 2000), while activation of the classical visual attention-related network constituting the posterior parietal cortex and the frontal eye fields (Goebel et al., 1998; Corbetta et al., 1998; Culham et al., 2001; Yantis et al., 2002) would decrease as the capacity limit is approached.

In the present fMRI study, we therefore used a delayed visual discrimination task with parametric variation of memory load from one to four objects. We presented complex nonnatural shapes that could not easily be verbalized in order to reduce the immediate accessibility of symbolic representations and increase the demand on visual attention. We expected to observe a monotonic increase of reaction times and drop of accuracy with increasing memory load and a dissociation of monotonic increases and inverted U-shape patterns of the BOLD signal according to the hypotheses laid out in the preceding paragraph.

## Materials and methods

### Subjects

All 12 subjects (eight male, four female) were right-handed and had no history of neurological or psychiatric disorder. The mean age was 27.3 years (SD: 2.4 years, age range: 24 to 31 years). All subjects gave written informed consent to participate in the study.

### Behavioral task

A delayed visual discrimination task was implemented on a personal computer using custom-developed software (Fig. 1A). Nonnatural objects (BORTS: blurred outlines of random tetris shapes), presented on the center of the computer monitor, were used as visual stimuli. One to four sample objects were presented for 500 ms each (*encoding* phase). Thus the length of the encoding phase varied between 500 and 2000 ms. After a delay of 12 s (*delay* phase), a test stimulus was presented for 2 s at the center of the monitor (*retrieval* phase). Subjects responded with a left- or right-hand button press to indicate a test that matched or did not match one of the sample objects. The intertrial interval lasted between 8 and 9.5 s, ensuring that a new trial would start every 24 s. The experiment was preceded by a training
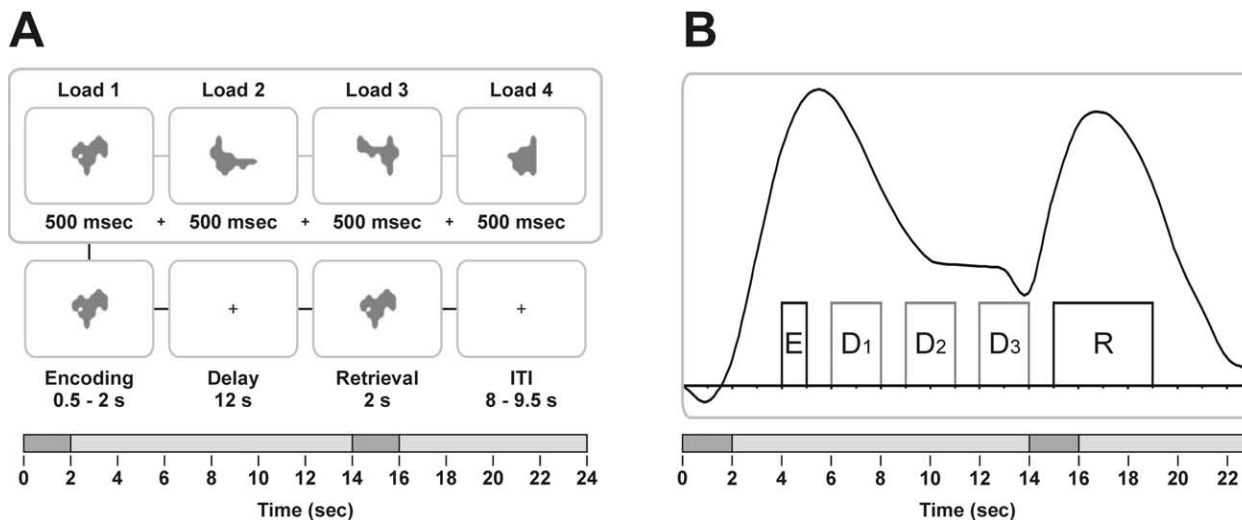
Fig. 1. Paradigm and design matrix. (A) The delayed visual discrimination task. Nonnatural objects (blurred outlines of random tetris shapes: BORTS) were used as stimuli. Load was varied by presenting one to four objects for 500 ms each for encoding. After a 12-s delay interval a probe stimulus was presented for 2 s and subjects had to judge by button press whether it was part of the sample set. (B) Predictors modeling the different task phases shifted by 4 s. The graph represents a paradigmatic time course from right IPS. E, encoding; $D_{1,2,3}$, early, middle, late delay; R, retrieval.

session which allowed subjects to complete as many trials as necessary to familiarize themselves with the structure and timing of the task. During scanning, the computer display was projected onto a mirror mounted on the head coil. Stimuli subtended 4° of visual angle. Subject's responses were registered by a custom-made fiber-optic response box. Subjects were asked to fixate upon the cross at the center of the monitor throughout the experiment. Each of the subjects completed 96 trials of the DDT (24 for each of the four memory load conditions) during fMRI data acquisition. Eye movement control was performed with separate electroencephalographic recording sessions on four of the subjects (for EEG/EOG parameters see Linden et al., 1999).

*Analysis of behavioral data*

Values for accuracy and reaction times were compared between memory load conditions with an analysis of variance (ANOVA). The number of stored items was calculated for individual behavioral data according to Pashler's method for estimating memory capacity (Pashler, 1988; Luck and Vogel, 1997),

$$s = n \cdot \frac{(h - g)}{(1 - g)},$$

with $s$ being the number of stored items, $n$ the number of items in the display (1 in memory load 1, 2 in memory load 2, etc.), $h$ the hit rate (correctly identified matches), and $g$ the rate of false alarms (nonmatches incorrectly identified as matches).

*fMRI scanning*

fMRI data were acquired with a Siemens 1.5-T Magnetom Vision MRI scanner using a gradient echo EPI sequence (8 axial slices; TR = 1000 ms; TE = 60; FA = 90°; FOV = 210 × 210 mm²; voxel size: 3.1 × 3.1 × 7 mm³). Functional images were acquired in four runs in a single session. Each run comprised the acquisition of 580 volumes and contained 24 trials (6 of each memory load condition). The slices covered large parts of the occipital, temporal, parietal, and frontal lobes ($z$ coordinate range from −5 to 45 at $y = -50$ and from 10 to 65 at $y = 20$, Talairach coordinates, Fig. 2A). Stimulus presentation was synchronized with the fMRI sequence at the beginning of each run. Each scanning session included the acquisition of a high-resolution T1-weighted three-dimensional (3D) volume (voxel size: 1 × 1 × 1 mm³) for coregistration and anatomical localization of functional data.

Fig. 2. Cortex-based group analysis of the experiment. (A) The analysis was restricted to the brain region commonly imaged in all 12 subjects (highlighted on each brain or flatmap). (B) Sulcal topography on the cortical flatmap of the MNI template brain used for visualization. CaS, Calcarine sulcus; CiS, Cingulate sulcus; CoS, Collateral sulcus; IFS, Inferior frontal sulcus; IPS, Intraparietal sulcus; LS, Lateral sulcus; MTS, Middle temporal sulcus; OF, Orbitofrontal sulci; OTS, Occipitotemporal sulcus; PCS, Postcentral sulcus; POS, Parietooccipital sulcus; RS, Rolandic sulcus; SFS, Superior frontal sulcus; STS, Superior temporal sulcus. (C–F) Superposition maps of the predictors modeling higher memory load conditions during encoding, delay, and retrieval. Effects were only shown if the associated $P$ value yielded $P' < 0.05$ (corrected for multiple comparisons). The three resulting 3D statistical maps were then projected on the flattened surface reconstruction of the MNI template brain. Each of the maps was associated with a color of the red–green–blue system (red: load 2; green: load 3; blue: load 4). Colors were superimposed and areas of overlap (cortical regions showing activation during more than one condition) received the appropriate mixed color.
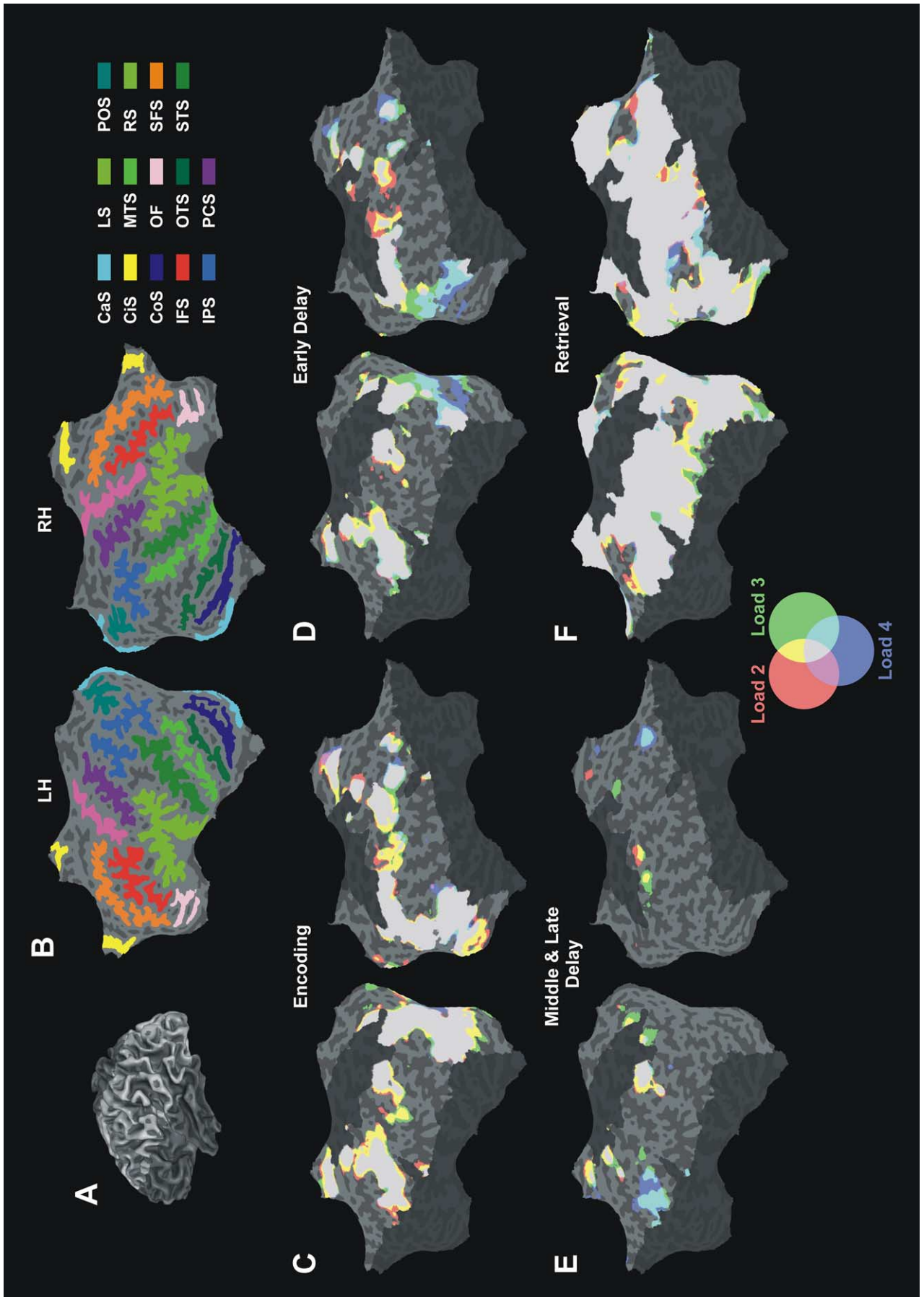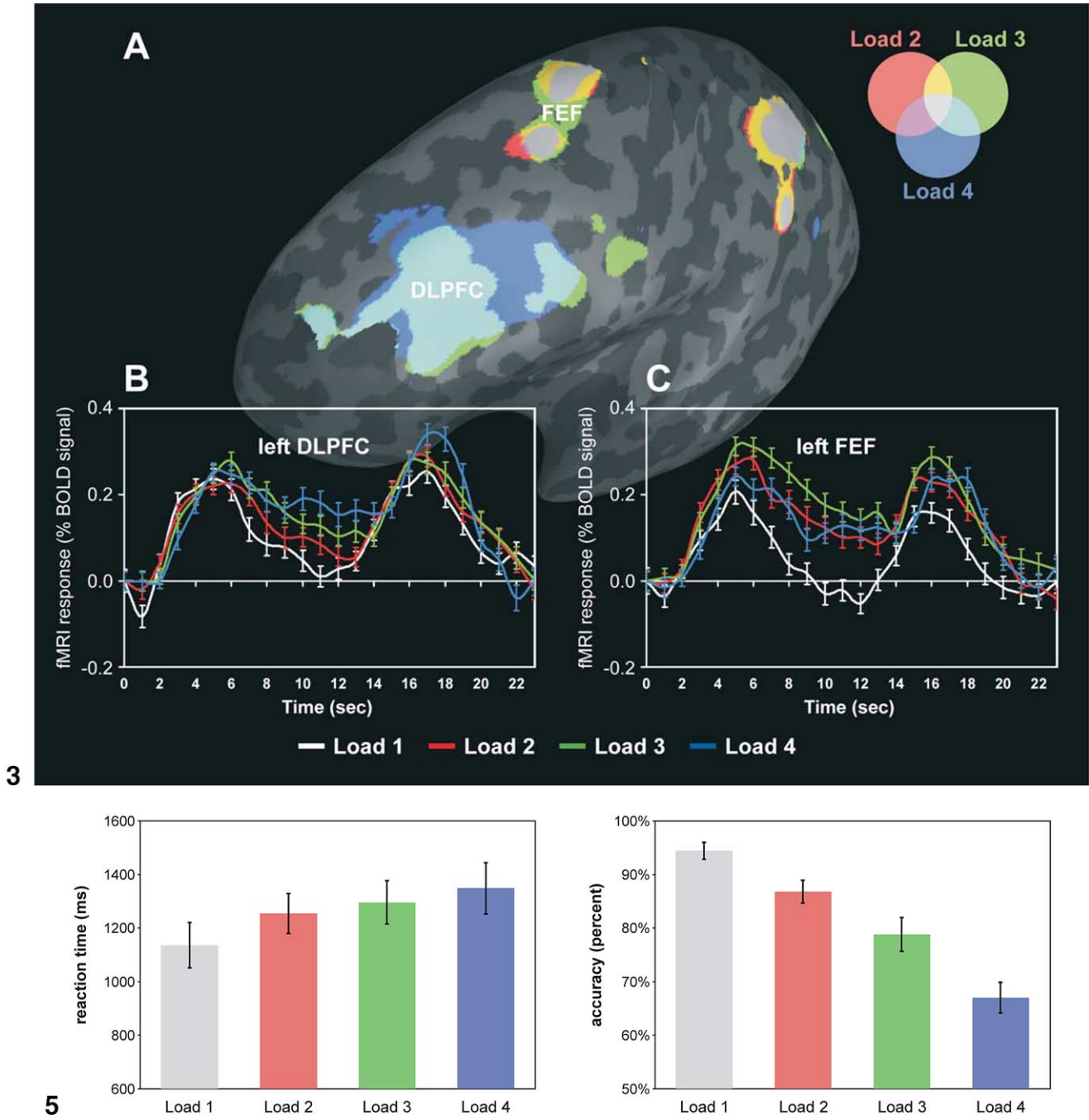
Fig. 3. Averaged time courses. (A) Regions of interests for which averaged time courses were derived. (B) Averaged timecourse of the left DLPFC representative for areas showing a load-dependent response. (C) Averaged time course of the left FEF representative for areas showing an inverted U-shape response. Conditions are coded as follows: load 1, white; load 2, red; load 3, green; load 4, blue. Error bars indicate standard error of the mean.
Fig. 5. Behavioral data. Reaction times and accuracy plotted against memory load conditions. Error bars indicate standard error of the mean.

*Data preprocessing and cortex-based statistics*

Functional data were preprocessed and analyzed using the BrainVoyager 4.9 package (www.brainvoyager.com). The first four volumes of each run were discarded to allow for T1 equilibration; 3D motion correction and Talairach transformation were performed for the remaining set of functional data of each subject. Data preprocessing further-more comprised spatial smoothing with a Gaussian kernel (FWHM = 8 mm) and temporal high pass filtering (high pass: 5 per functional run of 580 volumes). The cortical sheets of the individual subjects were reconstructed as polygon meshes based on the high-resolution T1-weighted structural three-dimensional recordings. The white–gray matter boundary was segmented, reconstructed, smoothed, and morphed (Kriegeskorte and Goebel, 2001). Based on the

gray–white matter boundary, a cortex mask for each subject was created that indexed all gray matter voxels. These 12 individual masks were then combined to produce a group mask.

The cortex-based general linear model (GLM) of the experiment was computed from the 48 (12 subjects, four runs per subject) z-normalized volume time courses. For each of the four memory load conditions five task phases were defined representing encoding, early, middle and late delay, and retrieval (Fig. 1B). The signal values during these phases were considered effects of interest. The corresponding predictors, obtained by shifting an ideal box-car response (assuming a value of 1 for the volumes of the respective task phase and a value of 0 for the remaining time points) by 4 s to account for the hemodynamic delay, were used to build the design matrix of the experiment. The delay phase was modeled by three predictors of 3 s duration each. This approach was chosen in order to avoid an overlap with the ascending slope of retrieval-related BOLD activity (Figs. 1B and 3). The retrieval phase was modeled by one predictor of 5 s (although test stimulus presentation was only 2 s) in order to cover the entire task period without gaps and to capture fully the BOLD response evoked by the test stimulus (Fig. 1$B$). The global level of the signal time courses in each session was considered to be a confounding effect, and a fixed effects analysis was employed. Effects are shown only if the associated $P$ value yielded $P' < 0.05$. The obtained $P$ values were corrected for multiple comparisons using a cortex-based Bonferroni adjustment, i.e., the number of comparisons considered was reduced by limiting the analysis to gray matter voxels, as defined by the group mask (Trojano et al., 2000; Muckli et al., 2002).

The resulting 3D statistical maps for the predictors of the higher memory load conditions (memory load 2–4) were projected on the flattened surface reconstruction of a template brain (courtesy of the MNI). Each of the maps was associated with a color of the red–green–blue (RGB) system (red: memory load 2; green: memory load 3; blue: memory load 4). Colors were superimposed and areas of overlap (cortical regions showing activation during more than one condition) received the appropriate mixed color (Fig. 2). The resulting superposition maps enabled us to display those areas particularly involved in the maintenance of multiple objects and to illustrate changes in the degree of activation and the extent of recruitment of these areas for the different memory load conditions and phases of the experiment. Four maps were created, showing activity during encoding, early delay, middle and late delay, and retrieval. Analysis of middle and late delay were combined in order to maximize statistical power for the detection of delay activity under the assumption that these predictors, in a box-car model like ours, capture activity uncontaminated by encoding or retrieval (Fig. 1B) (Zarahn et al., 1997; Rypma et al., 2002).

*Load response functions*

Load response functions were created for the cortical areas revealed by the superposition map of the middle and late delay predictors, i.e., those areas that were most closely associated with the maintenance of the stimuli. However, in order to assess the memory load-dependent activity at encoding in the inferior temporal cortex (which did not show sustained activity), the cluster selection for this area was based on the encoding map. The beta values of the encoding and all delay predictors (corrected for serial correlations) were plotted to visualize effects of memory load (Fig. 4). Contrasts between predictors of each memory load condition were calculated with Student's $t$ test ($P < 0.05$) (Table 1).

*Correlation with behavioral data*

The individual differences in the number of stored items in memory load conditions 3 and 4, as estimated with Pashler's equation, were correlated with the beta values of individual fMRI data sets (Pearson's correlation coefficient).

## Results

*Behavioral data*

For the behavioral data recorded during the experiment, the ANOVA revealed a significant main effect of memory load on reaction time and accuracy (Fig. 5) ($P < 0.05$). Accuracy decreased and reaction times increased monotonically with the number of objects. Reaction times were significantly longer for each increase in memory load. Accuracy was significantly lower for memory load 3 and 4 than for memory load 1 and 2. However, even in the highest memory load condition, accuracy was above chance level (mean accuracy 67.0%, SEM 10%), indicating that subjects were still engaged in the task. The number of stored items (mean of individual subjects/SEM) for the four memory load conditions was as follows: 0.93/0.09 (memory load 1); 1.60/0.26 (memory load 2); 1.91/0.54 (memory load 3); 1.90/0.97 (memory load 4).

*Eye movements*

Horizontal and vertical saccades >2° were detected and compared between memory load conditions. A Friedman test revealed no significant main effect of memory load (chi-square = 2.036; df = 3; $P = 0.565$). This result was confirmed by a Kendall–W test (Kendall–W = 0.170; df = 3; $P = 0.565$). Each possible combination of conditions was also compared using the Wilcoxon test, which showed no significant difference between any pair of conditions.

Table 1
Contrasts between the predictors documented in Fig. 4 (*P* values)

| | Left DLFPC | | | | | Right DLFPC | | | | |
|---|---|---|---|---|---|---|---|---|---|---|
| | Encoding | Early delay | Middle delay | Late delay | Retrieval | Encoding | Early delay | Middle delay | Late delay | Retrieval |
| 4 vs 3 | | | | | | | | | | |
| 4 vs 2 | | | *0.03* | 0.09 | | | 0.06 | *0.002* | *0.02* | |
| 3 vs 2 | | | 0.09 | 0.09 | | | | *0.009* | 0.06 | |
| 4 vs 1 | 0.07 | *$10^{-4}$* | *$10^{-5}$* | *0.02* | *0.01* | | *0.001* | *$10^{-5}$* | *0.02* | 0.06 |
| 3 vs 1 | *0.04* | *$10^{-5}$* | *$10^{-4}$* | *0.02* | *0.03* | *0.02* | *0.007* | *$10^{-4}$* | 0.08 | *0.04* |
| 2 vs 1 | 0.07 | *0.002* | *0.02* | | | | | | | |

| | Left pre-SMA | | | | | Right pre-SMA | | | | |
|---|---|---|---|---|---|---|---|---|---|---|
| | Encoding | Early delay | Middle delay | Late delay | Retrieval | Encoding | Early delay | Middle delay | Late delay | Retrieval |
| 4 vs 3 | | | 0.09 | *0.008* | | | | *0.002* | *0.005* | *0.05* |
| 4 vs 2 | | | | *0.02* | | | *0.03* | *0.005* | *0.009* | *0.03* |
| 3 vs 2 | | | | | | | | | *0.008* | *0.001* |
| 4 vs 1 | | *0.05* | *$10^{-5}$* | *$10^{-5}$* | *$10^{-5}$* | 0.09 | *$10^{-4}$* | *0.001* | | |
| 3 vs 1 | | 0.07 | *0.006* | *0.03* | *0.001* | | *0.008* | | | |
| 2 vs 1 | | | *0.003* | *0.02* | *0.001* | | 0.06 | | | |

| | Left FEF | | | | | Right FEF | | | | |
|---|---|---|---|---|---|---|---|---|---|---|
| | Encoding | Early delay | Middle delay | Late delay | Retrieval | Encoding | Early delay | Middle delay | Late delay | Retrieval |
| 4 vs 3 | | ***0.007*** | ***0.007*** | | ***0.01*** | | ***0.02*** | ***0.003*** | | ***0.01*** |
| 4 vs 2 | | **0.08** | | | ***0.005*** | | | | | ***0.002*** |
| 3 vs 2 | | | | | | | 0.09 | 0.02 | | |
| 4 vs 1 | | *0.005* | *0.002* | *0.002* | | *0.008* | *$10^{-6}$* | *$10^{-4}$* | *0.003* | |
| 3 vs 1 | | | *$10^{-5}$* | *0.002* | *0.03* | *$10^{-4}$* | *$10^{-6}$* | *$10^{-5}$* | *$10^{-5}$* | 0.09 |
| 2 vs 1 | 0.09 | | *$10^{-5}$* | *0.001* | *0.02* | *$10^{-4}$* | *$10^{-5}$* | *$10^{-5}$* | *0.001* | *0.03* |

| | Left IPS | | | | | Right IPS | | | | |
|---|---|---|---|---|---|---|---|---|---|---|
| | Encoding | Early delay | Middle delay | Late delay | Retrieval | Encoding | Early delay | Middle delay | Late delay | Retrieval |
| 4 vs 3 | | **0.09** | ***0.006*** | | | | | ***0.005*** | ***0.05*** | |
| 4 vs 2 | ***0.02*** | ***0.007*** | ***0.02*** | | | ***0.04*** | | **0.09** | | |
| 3 vs 2 | | | | | | | | | | |
| 4 vs 1 | | *0.02* | *0.002* | *0.009* | 0.09 | | *$10^{-5}$* | *0.001* | *0.05* | |
| 3 vs 1 | *0.006* | *$10^{-4}$* | *$10^{-5}$* | *0.001* | 0.08 | *0.003* | *$10^{-6}$* | *$10^{-6}$* | *$10^{-4}$* | *0.007* |
| 2 vs 1 | *$10^{-4}$* | *$10^{-5}$* | *$10^{-5}$* | 0.001 | *0.02* | *0.001* | *$10^{-6}$* | *$10^{-5}$* | *0.001* | *0.01* |

| | Left IT | | | | | Right IT | | | | |
|---|---|---|---|---|---|---|---|---|---|---|
| | Encoding | Early delay | Middle delay | Late delay | Retrieval | Encoding | Early delay | Middle delay | Late delay | Retrieval |
| 4 vs 3 | | | | | | | | | | |
| 4 vs 2 | *0.02* | *0.001* | *0.008* | | | *0.006* | *$10^{-5}$* | *0.03* | | |
| 3 vs 2 | | 0.06 | *0.05* | | | *0.01* | *0.002* | | | |
| 4 vs 1 | *$10^{-6}$* | *$10^{-5}$* | *0.002* | | | *$10^{-5}$* | *$10^{-5}$* | *0.002* | | |
| 3 vs 1 | *$10^{-5}$* | *$10^{-5}$* | *0.01* | | | *$10^{-5}$* | *$10^{-5}$* | *0.04* | | |
| 2 vs 1 | *$10^{-5}$* | *$10^{-4}$* | | | | *0.001* | *0.009* | | | |

*Note.* The contrasts that reached a $P < 0.1$ are documented. Significant values ($P < 0.05$) are reported in italics. *P* values in bold indicate that the beta weight was higher for the lower load condition.

### Encoding activity

The superposition map of the encoding predictors (Fig. 2C) shows activation in a widespread cortical network of early and higher visual areas that included the occipitotemporal and occipitoparietal pathways. Bilateral activation was also observed in the intraparietal sulcus (IPS), the frontal eye fields (FEFs), the supplementary motor area (SMA), and the prefrontal cortex.

### Delay activity

The superposition map of the early delay predictor (Fig. 2D) shows a pattern of activity very similar to encoding. A subset of the fronto-parietal network remained active during the middle and late delay, including the IPS, the left parieto-occipital sulcus (POS), the left supramarginal gyrus (SMG) and the right postcentral gyrus (PCS) in the parietal lobe, as well as the DLFPC, FEF, SMA, and pre-SMA bilaterally in
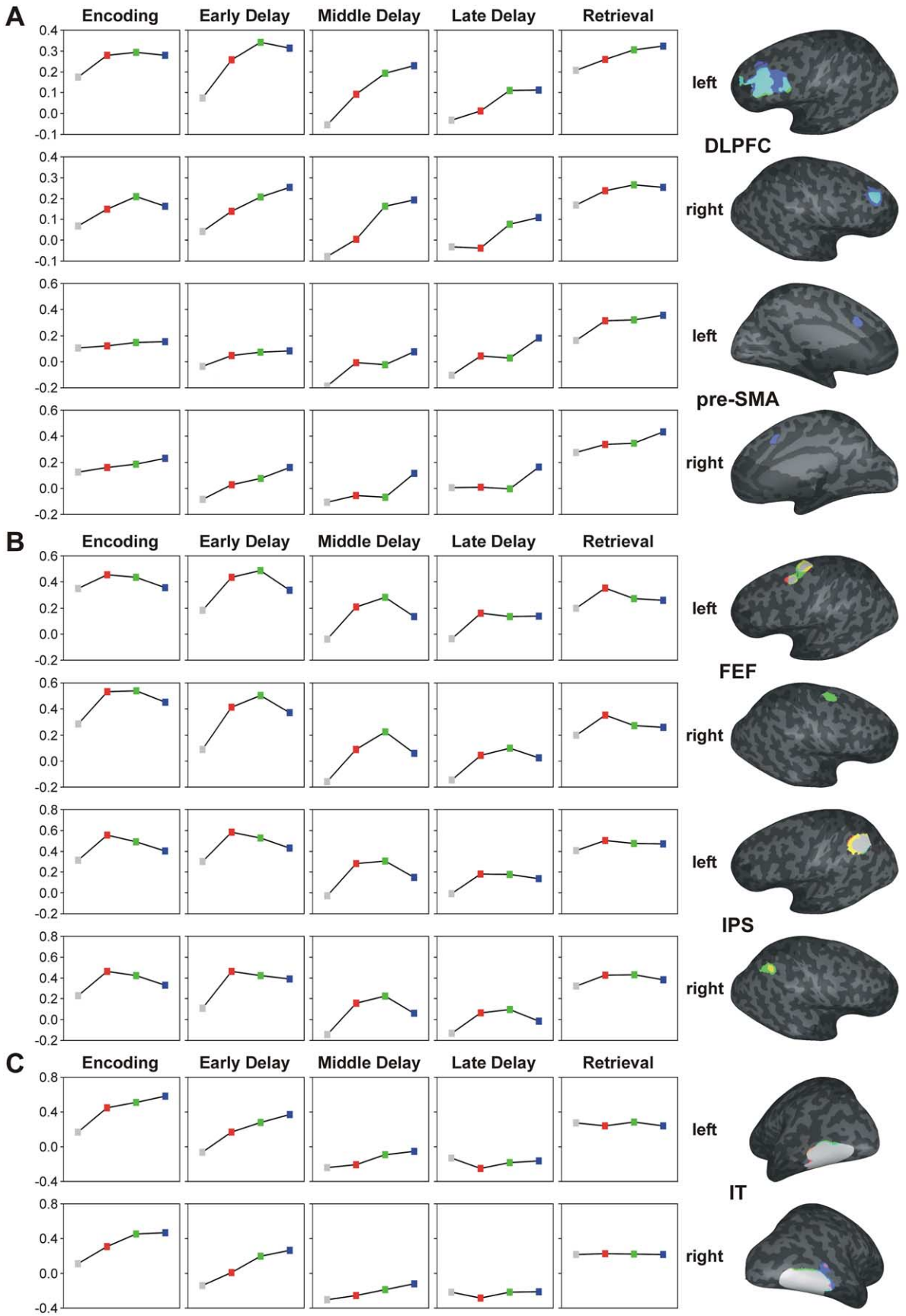
Fig. 4. Load response functions. (A) Response profiles of areas showing a load-dependent monotonic increase during delay. (B) Response profiles of areas showing an inverted U-shape response. (C) Response profiles of bilateral IT, showing a load-dependent monotonic increase mainly at encoding. Conditions are coded as follows: load 1, grey; load 2, red; load 3, green; load 4, blue. Regions of interest used for the generation of load response functions are shown on inflated cortical reconstructions of the MNI template brain. The extraction of these regions was based on the superposition maps of encoding (C) or middle and late delay, respectively (A and B).

Table 2
Talairach coordinates

| Region of activation | Left/right | From map | Cluster size (voxels) | Talairach coordinates (mm) | | | Brodmann area |
|---|---|---|---|---|---|---|---|
| | | | | $x$ | $y$ | $z$ | |
| IT | L | Encoding | 5867 | −40 | −64 | −6 | 19/37 |
| | R | | 5383 | 46 | −61 | 1 | 37 |
| DLPFC | L | Middle and late delay | 9546 | −37 | 15 | 30 | 9 |
| | R | | 1990 | 32 | 28 | 33 | 9 |
| FEF | L | | 2112 | −25 | −10 | 52 | 6 |
| | R | | 823 | 25 | −11 | 50 | 6 |
| Pre-SMA | L | | 164 | −6 | 17 | 41 | 6/32 |
| | R | | 173 | 8 | 12 | 37 | 6/32 |
| SMA | L | | 1905 | −6 | −2 | 49 | 6 |
| | R | | 265 | 10 | −4 | 42 | 6 |
| RS | L | | 394 | −49 | 4 | 30 | 4/6 |
| PCS | R | | 1096 | 33 | −34 | 40 | 2 |
| SMG | L | | 732 | −44 | −44 | 37 | 40 |
| IPS | L | | 2516 | −36 | −47 | 41 | 19/40 |
| | L | | 992 | −28 | −64 | 35 | 19 |
| | R | | 977 | 33 | −46 | 42 | 19/40 |
| POS | L | | 804 | −18 | −68 | 35 | 19 |

*Note.* Values are given for clusters from the middle and late delay surface map shown in Fig. 2 (and for the IT cluster from the encoding map).

the frontal lobe (Table 2). The color coding of the memory load conditions with significant beta values reveals a segregation of areas where more variance was explained by the memory load 4 predictor (DLFPC and pre-SMA bilaterally) and areas where more variance was explained by the memory load 2 or 3 predictors (parietal areas, FEF, SMA) (Table 1).

### Retrieval activity

The superposition map of the retrieval predictor (Fig. 2F) shows widespread activation in occipitotemporal, frontal, and parietal cortex. The prominent bilateral sensorimotor cortex activity is most probably related to the button presses.

### Load response functions

The load response functions (LRFs) revealed a principal difference in the amount of cortical activation between the single and multiple object conditions (Fig. 4). This was confirmed by the corresponding beta value contrasts (Table 1). Two main types of LRFs were identified: a memory load-dependent monotonic increase with a significant increase in activity beyond memory load 2 and a peak at memory load 4 (Figs. 4A and C), and an *inverted U-shape response* with a peak at memory load 2 or 3 and a significant decrease toward the highest memory load conditions (Fig. 4B). During encoding, a monotonic increase was observed most prominently in inferior temporal cortex (IT), while the parietal cortex and FEF demonstrated an inverted U-shape response. During delay, a monotonic increase was observed in the DLFPC and pre-SMA bilaterally, while an inverted U-shape response was found in IPS and FEF bilaterally. A

similar pattern was observed for retrieval. Selected time courses of BOLD signal change are shown for left DLFPC and left FEF (Fig. 3) in order to illustrate the time courses of memory load effects at finer temporal resolution.

### Correlation of BOLD signal and behavioral data

The correlation of the difference in stored items in memory load conditions 3 and 4 with that of the beta values at the single-subject level yielded a significant correlation ($P < 0.05$) or trend ($P < 0.1$) for left and right DLFPC and pre-SMA, mainly in the early delay. A negative correlation was observed for left and right FEF and IPS, mainly at encoding and during the middle and late delay. Finally a negative correlation in left and right FEFs, left IPS, and also left DLFPC was found for retrieval (Table 3).

### Discussion

The present study used a paradigm involving the manipulation of the number of non-natural objects that had to be stored in visual WM. We found that activity in the previously described fronto-parietal working memory network was consistently higher in the multiple than in the single object conditions, which conforms to the results of previous fMRI studies (Cohen et al., 1997; Jha and McCarthy, 2000). This effect was present at encoding and continued through the entire delay and retrieval period. However, the amplitude of the BOLD signal (represented by the beta weights of the general linear model of the experiment) did not increase monotonically with memory load in all of these areas. Our hypothesis was confirmed, in that we observed dissociation between cortical areas in which activity increased monoton-

Table 3
Correlation between behavioral data (change in number of stored items between load three and load four) and individual beta weights (*P* values)

|  | Encoding | Early delay | Middle delay | Late delay | Retrieval |
|---|---|---|---|---|---|
| Left DLPFC |  | 0.09 |  |  | ***0.04*** |
| Right DLPFC | **0.08** |  |  |  |  |
| Left pre-SMA |  | 0.06 |  |  | **0.09** |
| Right pre-SMA |  | *0.02* | *0.04* |  |  |
| Left FEF | **0.08** |  | **0.06** | *0.03* | *0.03* |
| Right FEF | **0.09** |  |  | *0.05* | *0.006* |
| Left IPS | *0.003* |  | **0.07** | **0.08** | **0.09** |
| Right IPS | *0.02* | *0.04* | **0.05** | **0.05** |  |
| Left IT |  |  |  |  |  |
| Right IT |  |  |  |  |  |

*Note.* Correlations that reached a *P* < 0.1 are documented. Significant values (*P* < 0.05) are reported in italics. *P* values in bold indicate a negative correlation.

ically and areas in which it declined as memory load increased beyond a certain level.

### Frontal cortex: DLFPC and pre-SMA

The middle frontal gyri and pre-SMA of both hemispheres showed an increase of the BOLD response with the number of presented objects beyond memory load 3 and thus did not appear to be influenced by supposed capacity constraints. It has been argued that the regions in lateral prefrontal cortex are likely to subserve the symbolic representation and executive processes required for working memory (Postle et al., 1999; Wagner et al., 2001). A recent study of verbal memory demonstrated increased activity in these areas as a correlate of memory organization processes that facilitated the maintenance of very large amounts of information (Rypma et al., 2002). Increasing prefrontal activation, in both lateral and mesial structures, has been shown previously in conditions of high integrative demand (Prabhakaran et al., 2000). In the highest memory load conditions of our study, subjects might have been forced to rely on the rehearsal of more integrated representations to compensate for their inability to retain the increasing amount of detail in the same manner as they managed to do in the easier conditions.

### Frontal cortex: FEF and SMA

The frontal regions showing a decrease in fMRI activity beyond memory load 3 (and thus an "inverted U-shape" response) were located along the precentral and superior frontal sulci (presumed site of the human FEF) and in the posterior part of the superior mesial frontal cortex (SMA). Both regions are believed to be part of the cortical system for directing visual attention (Corbetta et al., 1998) and have consistently been found to be active in studies of visual working memory (Postle et al., 2000; Munk et al., 2002). This overlap of cortical networks for visual attention and working memory has been taken as an indication that both cognitive processes rely on shared resources (LaBar et al.,

1999). There is indeed converging evidence from functional imaging and behavioral studies that selective attention is crucial for maintenance of information in visual working memory (Awh et al., 1998; Awh and Jonides, 2001; Wheeler and Treisman, 2002). Consistent with our hypothesis, we observed an inverted U-shape pattern of BOLD activity mainly in frontal and parietal (see below) attention-related regions and a negative correlation with performance. This might indicate that subjects reached a limit of their capacity to covertly scan the detailed visual features of the objects and consequently shifted to a different strategy, which relied more on the prefrontal regions that showed a continuing monotonic increase of the BOLD signal. This interpretation is supported by the observation that the inverted U-shape pattern, if present at all, started to manifest itself early in the task (encoding or early delay), indicating a failure of the initial scanning process (Fig. 4; Table 1).

### Parietal cortex

Like the FEF, various parietal regions, mainly along the IPS, showed an inverted U-shape pattern of BOLD activity in association with memory load. The IPS is another region where considerable overlap between attention and working memory-related activity has been demonstrated (LaBar et al., 1999). Several previous fMRI studies of working memory using nonnatural geometric stimuli similar to ours also reported substantial activation of parietal regions (Postle and D'Esposito, 1999; Nystrom et al., 2000). The IPS region is believed to play an essential role in the processing of spatial object representations in the absence of visual stimulation (Trojano et al., 2000; Sack et al., 2002; Formisano et al., 2002). The performance of working memory tasks with visual content certainly depends critically on this ability. Additionally, when multiple objects have to be maintained, the shifting of attention between different object representations becomes crucial, and both the FEF and the IPS have been shown to be highly involved in this process (Goebel et al., 1998; Culham et al., 2001). Thus, the pattern of activity observed in our study might very well reflect a rehearsal

procedure involving the repeated covert scanning of multiple objects. Such a strategy places great demands on the attention network. The observation of decreasing parietal activity in the memory load 4 condition compared to the memory load 3 condition during all phases of the delay suggests that both the initial scanning process and the attention-based rehearsal mechanism were affected by capacity limitation.

The absence of parietal inverted U-shape responses in earlier event-related functional imaging studies of WM load effects (e.g., Cohen et al., 1997; Jha and McCarthy, 2000; Leung et al., 2002) might be explained by the less complex visual characteristics of the stimuli used (e.g., letters). Also, the level of difficulty in these studies as indicated by both the number of items to be maintained and the accuracy of the participants was clearly below the level of difficulty in our study. Thus these studies most likely did not reach the capacity limit of working memory.

*Temporal cortex*

BOLD activity in IT was most prominent during the encoding phase and returned to baseline during the middle and late delay, confirming the results of earlier fMRI studies of DDT paradigms (Munk et al., 2002). A memory load-dependent monotonic increase was observed at encoding, indicating that the higher visual areas of the ventral stream, unlike those of the parietal lobe, were able to maintain the same level of visual information processing in the memory load 4 as in the memory load 3 condition. Why our study and most other fMRI studies of visual WM did not find sustained activity in the temporal lobe in contrast to single unit recordings (Miller et al., 1993) remains an open question.

*Correlation with behavioral data*

We interpret the dissociation of load effects as indicating that subjects compensated for the inability to retain the increasing amount of detail by shifting to more integrated representations. Such an interpretation is supported by the correlation analyses between BOLD signal time courses and measures of behavior, which showed that the number of items individual subjects were able to store correlated positively with activity in prefrontal areas during delay, while it was inversely correlated to activity in the FEF and parietal lobes. These results confirm previous studies that correlated prefrontal delay activity with subsequent memory performance and also found a positive correlation (Sakai et al., 2002; Pessoa et al., 2002; Rypma et al., 2002). This effect disappeared at retrieval when active rehearsal was no longer required. Instead, we observed a negative correlation between left DLPFC activity and performance. This latter effect is compatible with the observation by Rypma and D'Esposito (1999) that prefrontal retrieval activity is inversely correlated with retrieval performance.

## Conclusion

By analyzing the cortical BOLD responses associated with increasing memory load, we found evidence for correlates of capacity limitations in visual working memory. We observed dissociation between brain activity patterns in several prefrontal areas, in which activity continued to increase up to the maximum memory load condition of the paradigm, and regions of the visual attention network, in which activity started to decline as the behavioral capacity limit was approached. While these findings confirm the implicated role of attention as a cause of WM capacity constraints, the exact influence of attention on WM is not fully understood. Whether the limits of the attention network, as such, or rather those of the capacity for fronto-parietal cooperation (Sakai et al., 2002), constrain working memory capacity cannot be decided on the basis of the present data. However we were able to show that event-related fMRI can detect gradual changes in activity patterns within distributed cortical networks in response to increasing task demands. With fMRI we can thus study the neural correlates of cognitive capacity limitations. Further studies, combining behavioral and functional imaging techniques, will be needed to explore explicitly the interplay of attention and storage mechanisms in working memory.

## References

Awh, E., Jonides, J., 2001. Overlapping mechanisms of attention and spatial working memory. Trends Cogn. Sci. 5, 119–126.

Awh, E., Jonides, J., Reuter-Lorenz, P.A., 1998. Rehearsal in spatial working memory. J. Exp. Psychol. Hum. Percept. Perform. 24, 780–790.

Baddeley, A., 1992. Working memory. Science 255, 556–559.

Beauchamp, M.S., Petit, L., Ellmore, T.M., Ingeholm, J., Haxby, J.V., 2001. A parametric fMRI study of overt and covert shifts of visuospatial attention. NeuroImage 14, 310–321.

Braver, T.S., Cohen, J.D., Nystrom, L.E., Jonides, J., Smith, E.E., Noll, D.C., 1997. A parametric study of prefrontal cortex involvement in human working memory. NeuroImage 5, 49–62.

Callicott, J.H., Mattay, V.S., Bertolino, A., Finn, K., Coppola, R., Frank, J.A., Goldberg, T.E., Weinberger, D.R., 1999. Physiological characteristics of capacity constraints in working memory as revealed by functional MRI. Cereb. Cortex 9, 20–26.

Cohen, J.D., Perlstein, W.M., Braver, T.S., Nystrom, L.E., Noll, D.C., Jonides, J., Smith, E.E., 1997. Temporal dynamics of brain activation during a working memory task. Nature 386, 604–608.

Corbetta, M., Akbudak, E., Conturo, T.E., Snyder, A.Z., Ollinger, J.M., Drury, H.A., Linenweber, M.R., Petersen, S.E., Raichle, M.E., Van Essen, D.C., Shulman, G.L., 1998. A common network of functional areas for attention and eye movements. Neuron 21, 761–773.

Courtney, S.M., Ungerleider, L.G., Keil, K., Haxby, J.V., 1997. Transient and sustained activity in a distributed neural system for human working memory. Nature 386, 608–611.

Cowan, N., 2001. The magical number 4 in short-term memory: a reconsideration of mental storage capacity. Behav. Brain Sci. 24, 87–114.

Culham, J.C., Cavanagh, P., Kanwisher, N.G., 2001. Attention response functions: characterizing brain areas using fMRI activation during parametric variations of attentional load. Neuron 32, 737–745.

D'Esposito, M., Postle, B.R., Rypma, B., 2000. Prefrontal cortical contributions to working memory: evidence from event-related fMRI studies. Exp. Brain Res. 133, 3–11.

de Fockert, J.W., Rees, G., Frith, C.D., Lavie, N., 2001. The role of working memory in visual selective attention. Science 291, 1803–1806.

Formisano, E., Linden, D.E.J., Di Salle, F., Trojano, L., Esposito, F., Sack, A.T., Grossi, D., Zanella, F.E., Goebel, R., 2002. Tracking the mind's image in the brain. I. Time-resolved fMRI during visuospatial mental imagery. Neuron 35, 185–194.

Funahashi, S., Bruce, C.J., Goldman-Rakic, P.S., 1989. Mnemonic coding of visual space in the monkey's dorsolateral prefrontal cortex. J. Neurophysiol. 61, 331–349.

Fuster, J.M., Alexander, G.E., 1971. Neuron activity related to short-term memory. Science 173, 652–654.

Goebel, R., Linden, D.E.J., Lanfermann, H., Zanella, F.E., Singer, W., 1998. Functional imaging of mirror and inverse reading reveals separate coactivated networks for oculomotion and spatial transformations. Neuroreport 9, 713–719.

Haxby, J.V., Petit, L., Ungerleider, L.G., Courtney, S.M., 2000. Distinguishing the functional roles of multiple regions in distributed neural systems for visual working memory. NeuroImage 11, 380–391.

Jha, AP., McCarthy, G., 2000. The influence of memory load upon delay-interval activity in a working-memory task: an event-related functional MRI study. J. Cogn. Neurosci. 1 (Suppl 2), 90–105.

Kane, M.J., Bleckley, M.K., Conway, A.R., Engle, R.W., 2001. A controlled-attention view of working-memory capacity. J. Exp. Psychol. Gen. 130, 169–183.

Kriegeskorte, N., Goebel, R., 2001. An efficient algorithm for topologically correct segmentation of the cortical sheet in anatomical MR volumes. NeuroImage 14, 329–346.

LaBar, K.S., Gitelman, D.R., Parrish, T.B., Mesulam, M., 1999. Neuroanatomic overlap of working memory and spatial attention networks: a functional MRI comparison within subjects. NeuroImage 10, 695–704.

Leung, H.C., Gore, J.C., Goldman-Rakic, P.S., 2002. Sustained mnemonic response in the human middle frontal gyrus during on-line storage of spatial memoranda. J. Cogn. Neurosci. 14, 659–671.

Levy, R., Goldman-Rakic, P.S., 2000. Segregation of working memory functions within the dorsolateral prefrontal cortex. Exp. Brain Res. 133, 23–32.

Linden, D.E.J., Prvulovic, D., Formisano, E., Völlinger, M., Zanella, F.E., Goebel, R., Dierks, T., 1999. The functional neuroanatomy of target-

detection: an fMRI study of visual and auditory oddball tasks. Cereb. Cortex 9, 815–823.

Luck, S.J., Vogel, E.K., 1997. The capacity of visual working memory for features and conjunctions. Nature 390, 279–281.

Miller, E.K., Erickson, C.A., Desimone, R., 1996. Neural mechanisms of visual working memory in prefrontal cortex of the macaque. J. Neurosci. 16, 5154–5167.

Miller, E.K., Li, L., Desimone, R., 1993. Activity of neurons in anterior inferior temporal cortex during a short-term memory task. J. Neurosci. 13, 1460–1478.

Miller, G.A., 1994. The magical number seven, plus or minus two: some limits on our capacity for processing information. 1956. Psychol. Rev. 101, 343–352.

Muckli, L., Kriegeskorte, N., Lanfermann, H., Zanella, F.E., Singer, W., Goebel, R., 2002. Apparent motion: event-related functional magnetic resonance imaging of perceptual switches and States. J. Neurosci. 22, RC219.

Munk, M.H., Linden, D.E.J., Muckli, L., Lanfermann, H., Zanella, F.E., Singer, W., Goebel, R., 2002. Distributed cortical systems in visual short-term memory revealed by event-related functional magnetic resonance imaging. Cereb. Cortex 12, 866–876.

Nystrom, L.E., Braver, T.S., Sabb, F.W., Delgado, M.R., Noll, D.C., Cohen, J.D., 2000. Working memory for letters, shapes, and locations: fMRI evidence against stimulus-based regional organization in human prefrontal cortex. NeuroImage 11, 424–446.

Owen, A.M., 2000. The role of the lateral frontal cortex in mnemonic processing: the contribution of functional neuroimaging. Exp. Brain Res. 133, 33–43.

Pashler, H., 1988. Familiarity and visual change detection. Percept. Psychophys. 44, 369–378.

Pesaran, B., Pezaris, J.S., Sahani, M., Mitra, P.P., Andersen, R.A., 2002. Temporal structure in neuronal activity during working memory in macaque parietal cortex. Nat. Neurosci. 5, 805–811.

Pessoa, L., Gutierrez, E., Bandettini, P., Ungerleider, L., 2002. Neural correlates of visual working memory. fMRI amplitude predicts task performance. Neuron 35, 975–987.

Postle, B.R., Berger, J.S., D'Esposito, M., 1999. Functional neuroanatomical double dissociation of mnemonic and executive control processes contributing to working memory performance. Proc. Natl. Acad. Sci. USA 96, 12959–12964.

Postle, B.R., D'Esposito, M., 1999. "What"–then–"where" in visual working memory: an event-related fMRI study. J. Cogn. Neurosci. 11, 585–597.

Postle, B.R., Stem, C.E., Rosen, B.R., Corkin, S., 2000. An fMRI investigation of cortical contributions to spatial and nonspatial visual working memory. NeuroImage 11, 409–423.

Prabhakaran, V., Narayanan, K., Zhao, Z., Gabrieli, J.D., 2000. Integration of diverse information in working memory within the frontal lobe. Nat. Neurosci. 3, 85–90.

Ranganath, C., D'Esposito, M., 2001. Medial temporal lobe activity associated with active maintenance of novel information. Neuron 31, 865–873.

Rypma, B., Berger, J.S., D'Esposito, M., 2002. The influence of working-memory demand and subject performance on prefrontal cortical activity. J. Cogn. Neurosci. 14, 721–731.

Rypma, B., D'Esposito, M., 1999. The roles of prefrontal brain regions in components of working memory: effects of memory load and individual differences. Proc. Natl. Acad. Sci. USA 96, 6558–6563.

Rypma, B., Gabrieli, J.D.E., 2000. Functional neuroimaging of short-term memory: the neural mechanisms of mental storage. Behav. Brain Sci. 24, 143–144.

Sack, A.T., Sperling, J.M., Prvulovic, D., Formisano, E., Goebel, R., Di Salle, F., Dierks, T., Linden, D.E.J., 2002. Tracking the mind's image in the brain. II. Transcranial magnetic stimulation reveals parietal asymmetry in visuospatial imagery. Neuron 35, 195–204.

Sakai, K., Rowe, J.B., Passingham, R.E., 2002. Active maintenance in prefrontal area 46 creates distractor-resistant memory. Nat. Neurosci. 5, 479–484.

Smith, E.E., Jonides, J., 1999. Storage and executive processes in the frontal lobes. Science 283, 1657–1661.

Trojano, L., Grossi, D., Linden, D.E.J., Formisano, E., Hacker, H., Zanella, F.E., Goebel, R., Di Salle, F., 2000. Matching two imagined clocks: the functional anatomy of spatial analysis in the absence of visual stimulation. Cereb. Cortex 10, 473–481.

Ungerleider, L.G., Haxby, J.V., 1994. 'What' and 'where' in the human brain. Curr. Opin. Neurobiol. 4, 157–165.

Wagner, A., Maril, A., Bjork, R.A., Schacter, D.L., 2001. Prefrontal contributions to executive control: fMRI evidence for functional distinctions within lateral prefrontal cortex. NeuroImage 14, 1337–1347.

Wheeler, M.E., Treisman, A.M., 2002. Binding in short-term visual memory. J. Exp. Psychol. Gen. 131, 48–64.

Yantis, S., Schwarzbach, J., Serences, J.T., Carlson, R.L., Steinmetz, M.A., Pekar, J.J., Courtney, S.M., 2002. Transient neural activity in human parietal cortex during spatial attention shifts. Nat. Neurosci. 5, 995–1002.

Zarahn, E., Aguirre, G., D'Esposito, M., 1997. A trial-based experimental design for fMRI. NeuroImage 6, 122–138.